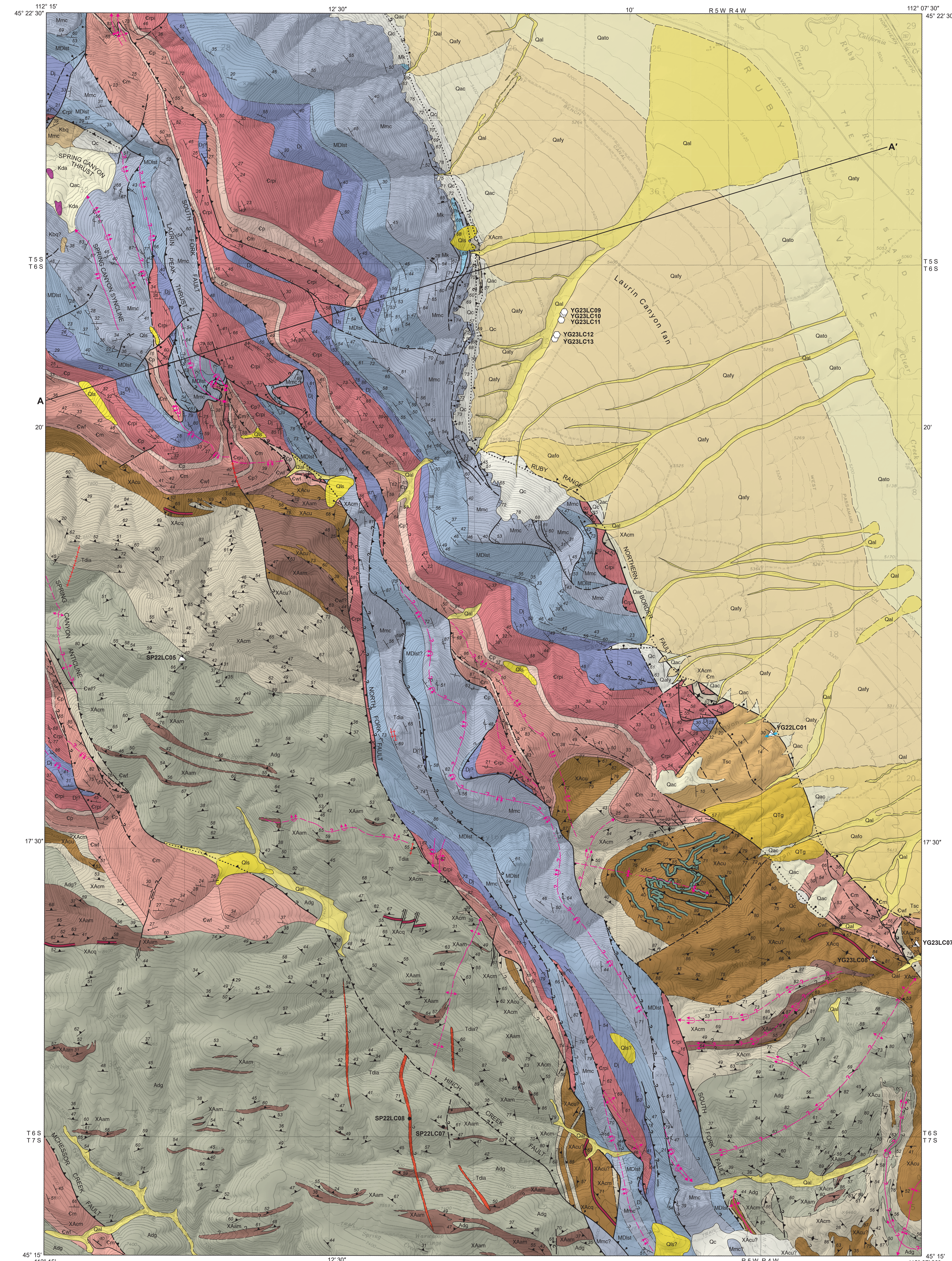

Base map produced by the United States Geological Survey Laurin Canyon 7.5′ 1:24,000-scale quadrangle map
Control by: USGS and USC&GC
Compiled from aerial photographs taken 1961
Field checked: 1963
Projection: Polyconic
Vertical Datum: National Geodetic Vertical Datum of 1929
Horizontal Datum: 1927 North American Datum

Shaded relief created from 10-meter digital elevation model from U.S. Geological Survey National Elevation Dataset.

SCALE 1:24,000

CONTOUR INTERVAL 40 FEET
NATIONAL GEODETIC VERTICAL DATUM OF 1929

Maps may be obtained from:
Publications Office
Montana Bureau of Mines and Geology
1300 West Park Street
Butte, Montana 59701-8997
Phone: (406) 496-4174
https://mbmg.mtech.edu

CORRELATION DIAGRAM

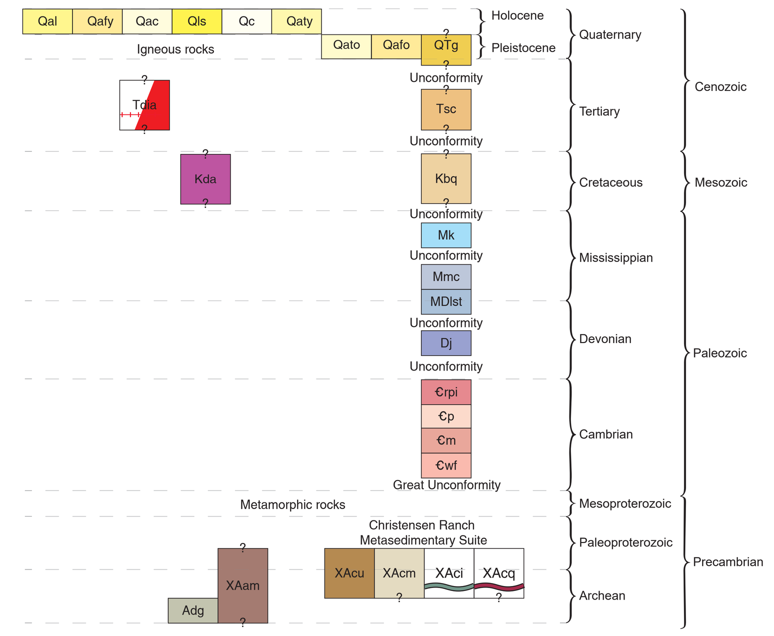

MAP SYMBOLS

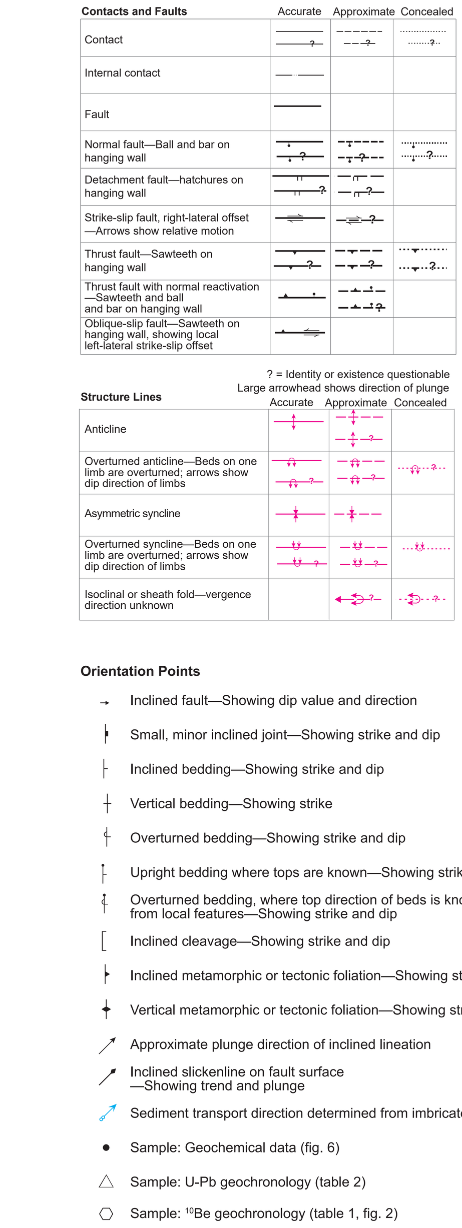

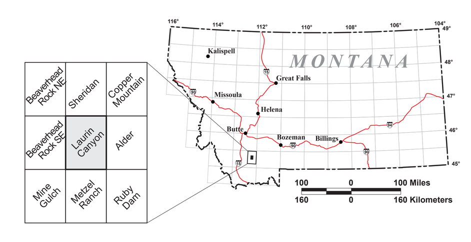

Cross Section A–A′

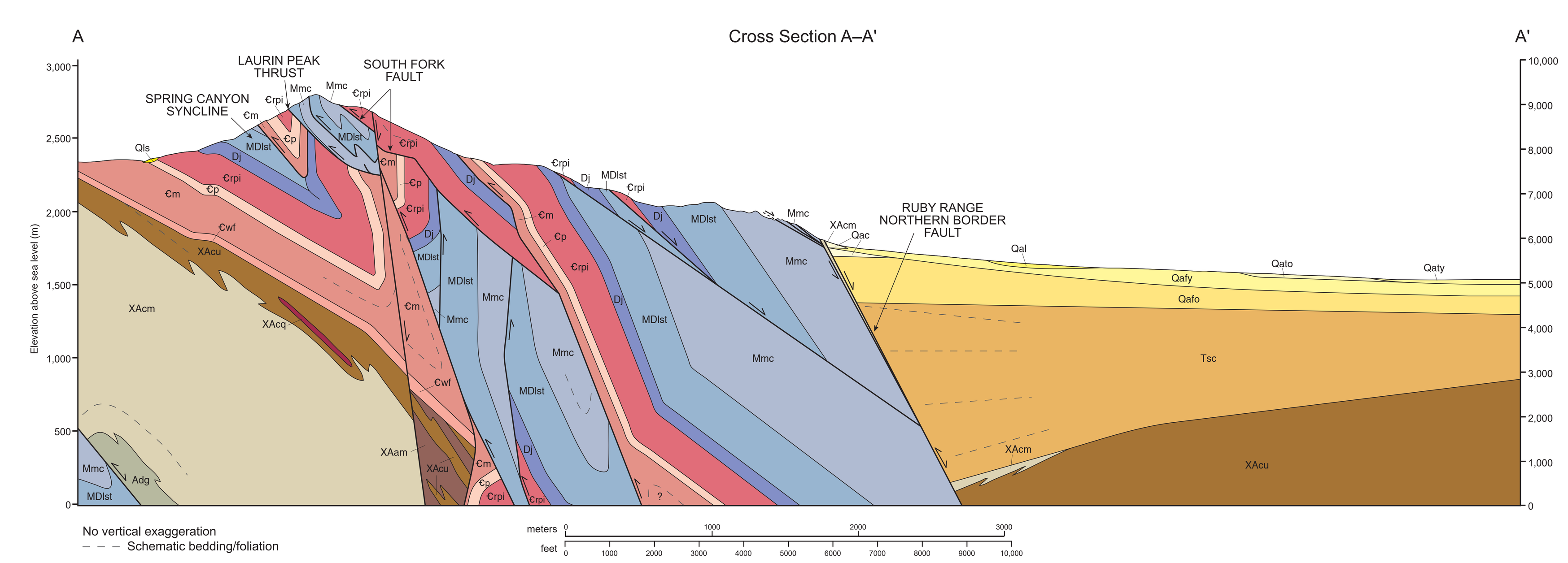

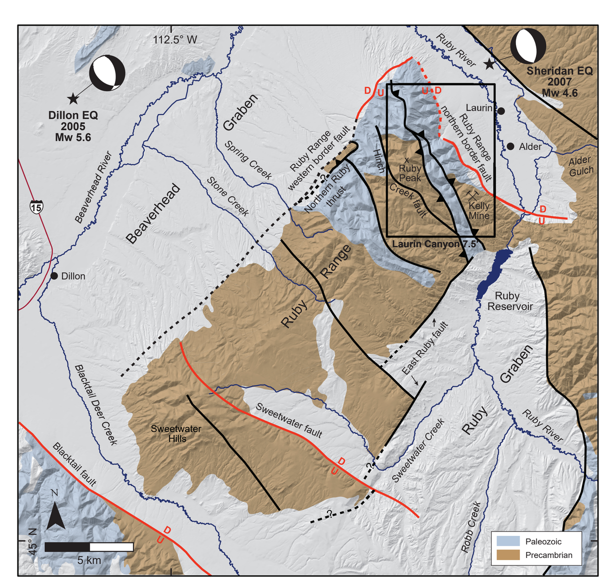

Figure 1. Simplified geologic map of the Ruby Range and surrounding area, showing the general geography and major faults. Extent of Paleozoic sedimentary rocks and Precambrian crystalline basement rocks shown. Laurin Canyon 7.5′ quadrangle shown in box. Normal faults with Quaternary displacement shown in red. Focal mechanisms shown for recent earthquakes with a magnitude of Mw >4.5.

Research supported by the U.S. Geological Survey, National Cooperative Geologic Mapping Program, under USGS award G22AC00376.
GIS production: Stuart Parker, Yann Gavillot, and Trish Ekberg, MBMG. Map layout: Susan Smith, MBMG. Editing: Susan Barth, MBMG.

INTRODUCTION

The Laurin Canyon 7.5′ quadrangle encompasses the northeast-facing range front of the northern part of the Ruby Range, in Madison County, Montana (fig. 1). Much of the mountainous terrain within the quadrangle is part of the Ruby Mountains Wilderness Study Area, with elevations ranging from 9,391 ft (2,862 m) at Ruby Peak, to around 5,000 ft (1,524 m) near the Ruby River. Lush wooded slopes of the northern part of the quadrangle have little to no running surface water due to the high permeability of the steeply dipping Paleozoic carbonate rocks. In contrast, open meadows of the southern part of the quadrangle contain flowing streams much of the year due to the impermeability of the underlying high-grade metamorphic basement rocks. The Great Unconformity marks the contact between Paleozoic sedimentary rocks and the underlying high-grade metamorphic basement rocks. Imbricated thrust sheets repeat the Paleozoic stratigraphy above the Great Unconformity (lower contact of Flathead Formation), while large fault blocks break the continuity of the underlying basement. Quaternary faulting associated with the Ruby Range northern border fault (fig. 1) controls the range front topography. Seismicity periodically occurs in the lower Ruby River Valley, near Sheridan and Laurin. The 2007 Mw 4.6 Sheridan earthquake damaged several masonry buildings, and occurred at a depth of 8.5 mi (13.6 km ± 0.4) on a normal fault that dips about 55–65° northeast, possibly on the northern border fault (fig. 1; Stickney, 2022). A major historic earthquake in 1897, with an estimated intensity magnitude of ~5.6 but poorly constrained epicenter location (± 50 km/30 mi), occurred in the vicinity of the northern Ruby Range (Stickney, 2022).

PREVIOUS MAPPING AND METHODS

Early work in the quadrangle focused on mapping the iron deposits of the Kelly Mine in the 1960s, which continued to receive attention for subsequent decades (James and Wier, 1961, 1972, scale 1:2,400; James, 1990, scale 1:4,600). Tysdal (1970, 1976) mapped the quadrangle at 1:24,000 scale, focusing on the Cambrian stratigraphy. Karasevich (1980; Karasevich and others, 1981) mapped the Precambrian basement in more detail (1:24,000 scale), describing multiple generations of ductile folding. Mapping of mineral resource potential, particularly talc, was conducted by the United States Geological Survey (USGS) as part of their assessment of the proposed Ruby Mountains Wilderness Study area (Tysdal and others, 1987, 1:24,000 scale). Several structural studies (e.g., Karasevich and others, 1981; Tysdal, 1981; Schmidt and Garihan, 1983; Schmidt and others, 1988) used these published maps of the northern Ruby Range in studies of regional tectonics. The Laurin Canyon 7.5′ quadrangle was included in small-scale maps (Ruppel and others, 1983, 1993, scale 1:250,000; St. Jean and Teeter, 2004, scale 1:48,000).

Rock samples collected by the authors for U-Pb geochronology were processed at the MBMG mineral separation laboratory. Zircon was isolated from selected samples by standard density and magnetic separation techniques. Zircon separates were analyzed by laser ablation inductively coupled plasma mass spectrometry (LA-ICPMS), at the University of California, Santa Barbara. All U-Pb data are reported in Mosolf and others (2023a), and Brennan and others (in prep.). Boulder samples collected by the authors for ^{10}Be cosmogenic radionuclides surface exposure dating were physically processed at the MBMG mineral separation laboratory. Quartz was isolated from selected samples using standard separation techniques for cosmogenic radionuclides dating. Quartz separates were sent to the Center for Accelerator Mass Spectrometry (CAMS), Lawrence Livermore National Lab, for further quartz purification, BeO chemical analysis, and measurement of ^{10}Be concentration via accelerator mass spectrometry (AMS). Modeled ^{10}Be cosmogenic radionuclides age results are shown in table 1 and figure 2.

GEOLOGIC SUMMARY

Highly deformed high-grade metamorphic rocks of the Archean to Paleoproterozoic Montana metasedimentary terrain are exposed throughout much of the southern part of the quadrangle (e.g., Harms and Baldwin, 2023). Several generations of deformation produced isoclinal to rootless folds, but the overall deformation pattern is consistent with general northwest–southeast shortening during the Big Sky Orogeny ca. 1.8–1.7 Ga (Harms and Baldwin, 2023). Unlike elsewhere in the Ruby Range, the basement rock's metamorphic fabric generally dips to the north. When the tilt of the overlying Cambrian rocks is restored to horizontal (fig. 3), Precambrian folds beneath the Great Unconformity plunge to the north. In the Ruby Range the basal contact of the Christensen Ranch Metasedimentary Suite follows the general northwest-dipping fabric of the Big Sky Orogeny, but in the northern part it apparently steps to the southeast by 2–3 mi (3–5 km). A thicker package of the Christensen Ranch Metasedimentary Suite is exposed below the Great Unconformity in the hanging wall of the Hinch Creek fault as compared to the footwall, suggesting down-to-the-northeast normal faulting in the Proterozoic (Schmidt and Garihan, 1983). By the middle Cambrian, erosion had exhumed these rocks and formed the Great Unconformity. In the map area, carbonate deposition occurred along the passive margin from the middle Cambrian to the Mississippian.

Rocks above and below the Great Unconformity were horizontally shortened during the Sevier–Laramide Orogeny. Above the Great Unconformity, bedding-parallel slip is common within Paleozoic sedimentary rocks, accommodating folding and thrust faulting. The Great Unconformity appears sheared near South Fork Canyon. Near the center of the map, from east of Ruby Peak to Hinch Creek, a strip of steeply dipping Mississippian rock units is bounded between the opposite-verging North Fork and South Fork faults. Crosscutting relationships suggest that deformation progressed from west to east. Thrust reactivation of the northeast-dipping McHessor Creek and Hinch Creek faults was followed by slip on the east–northeast-verging North Fork thrust fault. Slip on the North Fork fault diminishes in a fault-propagation fold north of Laurin Canyon, where the fault–fold pair is truncated by the low-angle Laurin Peak thrust, resulting in local younger-on-older relationships. Kinematic analysis of slickenlines within small splays of the Laurin Peak thrust (fig. 4) suggest that slip was directed toward the west–southwest (259 ± 17°), orthogonal to the broken Spring Canyon syncline. The Laurin Peak thrust is a footwall imbricate to the South Fork fault, the youngest thrust fault in the quadrangle. During top to the west–southwest slip on the South Fork fault, rocks in the footwall and the North Fork fault were rotated to near vertical.

A dike north of Ruby Peak intrudes a normal fault that offsets Paleozoic rocks, suggesting a Tertiary age. At least two generations of dikes are present in the Ruby Range; Mesoproterozoic dates have been documented to the south (Wooden, 1975). Across the Hinch Creek fault, a large dike and the North Fork fault show apparent right-lateral offset, but the Great Unconformity shows apparent left-lateral offset. This relationship is consistent with Cretaceous thrusting followed by dike emplacement and subsequent normal reactivation of the Hinch Creek fault, as has been proposed elsewhere in the Ruby Range (Schmidt and Garihan, 1983). Isolated exposures of basement rock along the trace of the Ruby Range northern border fault also suggest reactivation of an older thrust fault during Cenozoic extension (see cross-section).

Cenozoic normal faults have since dissected the compressional features, particularly the Ruby Range northern border fault, which defines the prominent active range front with a topographic escarpment that bounds the western edge of the southern Ruby River Valley below the reservoir. Fault scarps, truncated alluvial fan deposits, and range front triangular facets suggest Quaternary displacement on the Ruby Range northern border fault. Deformed older alluvial fans (Qafo) south of Laurin Canyon suggest that Quaternary fault movement occurred within the past 130,000 years. North of Laurin Canyon the Ruby Range northern border fault exhibits triangular facets, but the trace of the fault is concealed by rock talus colluvium (Qc). The western edge of the Laurin Canyon fan complex (Qafy) follows the trend and topographic break of the concealed Ruby Range northern border fault. ^{10}Be cosmogenic radionuclides surface exposure dating from five boulders collected on the Laurin Canyon fan yielded a model age of 37.8 ± 0.7 ka (table 1, fig. 2), and suggest fault displacement on the Ruby Range northern border fault occurred since deposition and surface abandonment of the Laurin Canyon Fan in the past 40,000 years. The Ruby Range northern border fault was initially inferred and mapped as an approximately 22-km-long Quaternary fault by Stickney and others (2000) and is included within the USGS Quaternary Fault and Fold Database. Fault slip rates are unconstrained, but estimated to be less than 0.2 mm/yr, similar to other potential seismogenic faults in southwestern Montana (Stickney and others, 2000). The USGS earthquake scenario forecast indicates a magnitude 6.6 earthquake is possible within the lower Ruby Valley (https://earthquake.usgs.gov/scenarios/eventpage/mt2016montana_666_se/executive).

DESCRIPTION OF MAP UNITS

Qal **Alluvium (Holocene)**—Unconsolidated, poorly sorted to well-sorted gravel, sand, silt, and clay deposited by modern streams and rivers. Thickness generally less than 15 ft (5 m), but as thick as 30 ft (10 m) within the channel thalweg.

Qafy **Younger alluvial fan deposits (Holocene)**—Unconsolidated deposits of clay- to boulder-sized angular to subangular clasts forming broad incised surfaces along modern drainages. Deposited as coalescent alluvial fan channels to debris-flow fans along steep range fronts. Surfaces of these deposits stand at lower levels and shallower slopes than older alluvial fans. Surface exposure dating on five quartzite boulders using cosmogenic ^{10}Be yielded a surface abandonment age that ranges between 35.3 ± 1.4 ka and 46.8 ± 2.0 ka, with a combined model age of 37.8 ± 0.7 ka (table 1, fig. 2). As thick as 30 ft (10 m) at the surface but inferred to be up to about 300 ft (90 m) in the subsurface.

Qac **Alluvium and colluvium (Holocene)**—Dominantly sand, silt, clay, and subordinate gravel locally, deposited on relatively gentle slopes primarily by sheetwash and gravity processes. Thickness generally less than approximately 30 ft (10 m).

Qls **Landslide deposit (Holocene)**—Mass-wasting deposit that consists of unsorted mixtures of clay- to boulder-sized sediment. Color and lithology reflect that of nearby parent rocks and transported surficial material. Variable thickness, typically less than approximately 100 ft (30 m).

Qc **Colluvium (Holocene)**—Unconsolidated, subangular gravels with local boulders, deposited on hillslopes as debris flows, rock falls, and mass movement. Thickness generally less than approximately 30 ft (10 m).

Qaty **Younger alluvial terrace (Holocene)**—Unconsolidated, poorly sorted to well-sorted gravel, sand, silt, and clay deposited as fluvial terraces along active channels. Thickness generally less than 16 ft (5 m).

Qato **Older alluvial terrace (Pleistocene)**—Unconsolidated, poorly sorted to well-sorted gravel, sand, silt, and clay deposited as terraces associated with older fluvial to alluvial deposits of the Ruby River that form surfaces elevated above younger fluvial terraces (Qaty). Thickness generally less than approximately 30 ft (10 m).

Qafo **Older alluvial fan deposit (Pleistocene)**—Unconsolidated deposits of clay- to boulder-sized angular to subangular clasts forming broad incised surfaces along modern drainages. Deposited as coalescent alluvial fan channels and debris-flow fans along steep range fronts. Surfaces of these deposits are elevated above younger alluvial fans and are steeper. A good exposure of a younger alluvial fan incising an older alluvial surface occurs south of Laurin Canyon (sec. 11 T. 6 S., R. 5 W.). Variable thickness, with a maximum of at least 30 ft (10 m) thick where exposed but inferred to be up to about 300 ft (90 m) in the subsurface.

QTg **Gravel (Pleistocene? to Miocene?)**—Unconsolidated deposits of cobble- to boulder-sized subangular to angular clasts forming highly dissected weathered surfaces. These surfaces appear as pediments on the older Sixmile Creek Formation (Tsc) or older Quaternary gravels. At least 30 ft (10 m) thick.

Tdia **Diabase dike (Tertiary?)**—Dark brown to gray, red- to dark tan-weathering fine- to medium-grained diabase (50.5 wt. percent SiO_2, fig. 6; Mosolf and others, 2023b). Commonly ophitic texture with coarse white plagioclase laths in pyroxene groundmass. One dike, northwest of Ruby Peak, contains abundant olivine and pyroxene, with no visible plagioclase laths. Nine samples from the Ruby Range have an average whole-rock geochemical composition of tholeiitic basalt (Wooden, 1975). In the southwestern Ruby Range, six northwest–southeast-striking dikes yielded a whole-rock Rb-Sr isochron age of 1,455 ± 125 Ma (Wooden, 1975). Dikes in the study area strike north–south (± 30°), suggesting they are of a different age. Tertiary age is speculative, based on field observations (see geologic summary). Dikes are meters to tens of meters wide, and up to about 1 mi (2 km) long.

Tsc **Sixmile Creek Formation (Pliocene? to early Tertiary?)**—Indurated conglomerate with silica cement, subangular to angular pebbles, coarse sand to cobbles and boulders derived primarily from basement clasts and subordinate Paleozoic carbonates. Locally, white fine sandstone with little to no gravel is intercalated with the conglomerate, with cross-beds, laminations, and soft sediment deformation. Unit exposed along the eastern range front of the Ruby Range. Sandy ash beds near the Ruby Range northern border fault yielded U-Pb zircon dates with a weighted mean of 8.0 ± 0.1 Ma (table 2, fig. 5; Mosolf and others, 2023a). Previously mapped as Upper Bozeman Group (?) (Miocene to Pliocene) by Tysdal (1976). Total thickness unknown but is at least 130–160 ft (40–50 m) thick.

Kbq **Quartzite conglomerate member of the Beaverhead Group (Late Cretaceous)**—Indurated conglomerate in dark brownish-red sand matrix and locally coarse sandstone beds, well-rounded fluvial pebbles to boulder-sized quartzite clasts, likely derived primarily from Belt Supergroup rocks. Contains subordinate clasts of basement gneiss and Paleozoic carbonates. Unit exposed along the western range front of the Ruby Mountains. At least 400 ft (120 m) thick.

Kda **Dacite (Late Cretaceous?)**—Black, brown-red-weathering porphyritic to vesicular dacite. Fine-grained pyroxene, and plagioclase phenocrysts are common. Phenocrysts are often weathered out, leaving behind angular voids. Exposed near Spring Canyon, where outcrops form a small linear ridge that is mostly concealed by surficial deposits. Age and rock type are tentative, based on lithologic similarities with a 72 Ma dacite dated in the neighboring quadrangle (Mosolf and others, 2023a, b), about 1 mi (1.5 km) west of the map boundary. Thickness unknown.

Mk **Kibbey Formation (Mississippian)**—Maroon to light gray, red-weathering fine-grained muddy quartz arenite and interbedded lavender micrite with platy centimeter-scale bedding. Crude, low-relief channels and cross-beds are common. Rarely exposed, more commonly forming red slopes. Conodonts suggest a late Mississippian (Meramecian) age (Sando and Sandberg, 1985). At least 140 ft (43 m) thick based on measured section in Dry Creek, in the neighboring Beaverhead Rock SE 7.5′ quadrangle (Tysdal, 1970).

Mmc **Mission Canyon Formation (Mississippian)**—Light gray-weathering, massive cliff-forming limestone. Sparry cement often obscures primary crinoidal packestone lithology. Commonly brecciated. Upper part superficially resembles the Lodgepole Formation, with tabular crystalline limestone beds and bedded to nodular chert. Contact placed at the lowest cliff of massive limestone. Upper contact not constrained in quadrangle, but unit appears to be at least about 925 ft (280 m) thick along the range front.

MDlst **Lodgepole, Sappington, and Three Forks formations, undivided (Mississippian to Devonian)**—
Lodgepole Formation—Gray to lavender tabular-bedded micrite and wackestone, with yellow silty partings, grades downward into laminated gray to lavender micrite with thin continuous to stringy discontinuous orange-brown-weathering chert beds. Tabular bedding dominates, on the centimeter- (1 in) to decimeter- (6 in) scale, particularly in the upper part. Upper part contains highly fossiliferous wackestone beds with sharp scoured bases which fine up into micrite with silty parting containing abundant bed parallel trace fossils and *Zoopyhcos*. Intact crinoids, fenestrate bryozoan, bivalves, and disarticulate brachiopods including *Orthotetes* are common, especially near the top of the unit. Mostly covered by talus slopes, with platy to chippy float characterizing the lower part. Upper contact is placed below first massive cliff-forming limestone of the Mission Canyon Formation. Internal contact mapped where lower contact is confidently placed, at the lowest laminated micrite bed. Early to Middle Mississippian (Kinderhookian to Osagean) in age (Sando and Dutro, 1974). Thickness about 700 ft (215 m).
Sappington Formation—Yellow-weathering partly calcareous siltstone to very fine sandstone. Latest Devonian (late Famennian) in age (di Pasquo and others, 2017). Not exposed, except in Bogue Canyon where it has a measured thickness of about 70 ft (20 m; di Pasquo and others, 2017).
Three Forks Formation—Light mint green to deep red chippy mudstone, siltstone, and breccia and light gray-brown, orange-weathering micrite with mud chip breccia. Rarely exposed. These lithologies likely belong to the Logan Gulch Member, in the lower part of the unit. Uncommon silty limestone exposures, such as near Robinson Canyon, may belong to the Trident Member or the Knoll limestone at the top of the Logan Gulch Member (Sandberg, 1965). Latest Devonian (early to middle Famennian) in age (di Pasquo and others, 2017). Thickness is poorly constrained, but is likely around 80 ft (25 m).

Dj **Jefferson Formation (Devonian)**—Gray to bleached white tabular-bedded crystalline dolostone. Recessive with sparse outcrops, often with "elephant skin" weathering. Pervasive secondary dolomite obscures much of the original sedimentary structure, although mottled textures remain common. Brown brecciated dolostone beds are uncommon. Where secondary dolomite is minimal, bedsets of tabular dolostone alternate from thin-bedded and laminated to thick-bedded and mottled, with rare graded bedding and mud chips. A marker unit of cliff-forming, very thick (3–6 ft, 1–2 m) tabular bedded vitreous white dolostone occurs near the base of the unit in many places. Lower contact is placed below the lowest pure dolostone bed, and above the siliciclastic intervals. Upper contact is placed above highest dolostone bed, below the lowest slope of chippy limestone or siltstone float. Likely Late Devonian in age, based on regional correlations (e.g., Dorobek and others, 1991). Thickness is about 245 ft (75 m) near Laurin Peak.

Ꞓrpi **Red Lion and Pilgrim formations, undivided (upper Cambrian)**—Tan, tabular to massive grainy weathering dolostone, gray to tan wavy thin-tabular bedded ("ribboned," Tysdal, 1970) dolo-wackestones with pale green to red silty partings and rare cross-bedded quartz arenite with dolomite cement. Laminated and mottled beds common, recrystallized dolomite mudchips uncommon. Lower portion forms prominent cliffs and is carbonate rich. Upper portion contains more siliciclastic material, including "ribbon rock." Cross-bedded sandstone is a marker unit, near the upper part. Ribbon rock varies from graded dolostone beds with trace amounts of siliciclastics, to red graded very fine sandstone to siltstones, with rippled muddy partings and extensive bioturbation. Gradational contacts separate these lithologies at multiple stratigraphic positions, and along-strike changes in thickness and lithology are common. A 2 ft (<1 m) bed of green shale is rarely observed, in sharp contact below ribbon rock, interpreted by Tysdal (1970) as a sequence boundary marking the base of the Dry Creek Member of the Red Lion Formation. However, in much of the quadrangle the shale is absent, and ribboned rock occurs both above and below the cross-bedded sandstone marker. Therefore, the Red Lion Formation may largely be absent in the quadrangle, except where the internal contact of the shale member has been mapped. Lower contact is marked by the lowest outcrop of dolostone. Upper contact is placed below first resistant thick-bedded bleached crystallized dolomite bed of the Jefferson Formation. Age is likely upper Cambrian based on correlative strata in southwestern Montana (e.g., Bush and others, 2012; Link and others, 2017). A thickness of 560 ft (170 m) was measured in McHessor Creek (Tysdal, 1970).

Ꞓp **Park Formation (middle Cambrian)**—Green shale and rare brown to tan limestone pebble conglomerate. Rarely crops out, and more commonly forms soft, recessive slopes of green to maroon shale with gray-lavender to orange micrite, and rare red oncoid limestone float. Common detachment surface for landslides. Fossils collected in the quadrangle suggest a middle Cambrian age (Tysdal, 1970). Measured section just south of Laurin Peak is 197 ft (60 m) thick (Tysdal, 1970).

Ꞓm **Meagher Formation (middle Cambrian)**—Mottled red- to tan-weathering sparry dolomite in gray fine-grained limestone micrite, and heavily recrystallized dolostone packestones and ooid grainstones. Characteristic mottled lime–dolostone intervals are more common in lower half. Micrite laminations, ooids, pisoids, and mud chips common but difficult to see due to grainy dolomite recrystallization of mud. Heavily bioturbated, including branching centimeter-scale burrows (twiggy forms of Tysdal, 1970). Bedding is commonly thin, wavy tabular, to meter-scale planar tabular with pronounced light and dark gray mottling. Lower part often forms talus slopes, with upper part forming prominent cliff bands. Fossils collected in the quadrangle suggest a middle Cambrian age (Tysdal, 1970). The only complete, unfaulted section occurs south of Laurin Peak, where the total thickness is 565 ft (172 m; Tysdal, 1970).

Ꞓwf **Wolsey and Flathead formations, undivided (middle Cambrian)**—
Wolsey Formation—Green, papery micaceous shale rarely outcrops, and more often forms swales with rare green chippy shale float. Internal contact between Flathead and Wolsey only shown where precisely known. Upper contact placed at base of talus slope of lower Meagher. Variable thickness, with 47 ft (14 m) measured south of Laurin Peak (Tysdal, 1970).
Flathead Formation—Tan, orange- to red-weathering medium-grained quartz arenite. Ranges from fine to very coarse, sometimes micaceous or glauconitic, moderately to well-sorted with subrounded to well-rounded, sometimes frosted grains. Bedding is commonly tabular to massive or trough cross-bedded, with rare meter-scale foresets and ripples. Rare vertical burrows. Lower contact is Great Unconformity. Thick cliffs, like in Taylor Creek, may be repeated by small thrust faults near the Great Unconformity. Age of both units is likely middle Cambrian (e.g., Thomas, 2007; Bush and others, 2012). Variable thickness, with 58 ft (18 m) measured just south of Laurin Peak (Tysdal, 1970).

Christensen Ranch Metasedimentary Suite (CRMS)

XAcu ***Undifferentiated metasedimentary rocks (Paleoproterozoic to Archean?)***—A variety of predominantly metasedimentary rocks including marble, quartz–biotite–garnet and rare phlogopite–sillimanite–garnet schist, and vitreous white to green micaceous quartzite and schist with uncommon biotite and garnet. Plagioclase–hornblende–diopside gneiss with uncommon biotite and garnet is a key marker unit near the Kelly Mine area (James, 1990). While these lithologies are distinctive for the suite, the most abundant lithologies are intermediate to felsic quartzofeldspathic gneiss with uncommon garnet and amphibolite. The type section at Sorensen Ranch occurs in the nearby Christensen Ranch quadrangle, about 9 mi (15 km) southwest of the map area (James, 1990). While a thick marble unit reliably marks the base of the suite throughout the region (Jones, 2008), it is typically bounded on both sides by quartzofeldspathic gneiss and amphibolite, making it difficult to differentiate the CRMS from the Dillon Gneiss without exposures of more characteristic metasedimentary lithologies. Near the type locality, U-(Th)-Pb dating of monazite within schist, amphibolite, and gneiss yielded ages of peak metamorphism at ca. 1.75 to 1.81 Ga (Jones, 2008; Cramer, 2015). U-Pb dating of zircon from two quartzofeldspathic gneiss samples within the map area yields older age populations of ca. 2.44 and 3.22 Ga (figs. 7A, 7B), suggesting Paleoproterozoic metamorphism or deposition. Apparent thickness of at least 2,000 ft (600 m) on the north flank of Ruby Peak.

XAcm ***Marble (Paleoproterozoic? to Archean?)***—White to gray, tan- to brown-weathering medium to coarsely crystalline dolomitic and calcitic marble. Ranges from massive to weakly foliated, often forming moderately resistant outcrop bands. Magnetite, diopside, and boudins of quartzite are common. Phlogopite and tremolite are uncommon, in impure layers. Dolomitic beds tend to be thicker, cleaner, and more monomineralic, while calcitic beds are thinner, more isolated, and with more calc-silicate minerals. Talc is also common in coarse dolomite marble, particularly near Ruby Peak (Tysdal and others, 1987). Lower contact with the Dillon Gneiss is very sharp near Ruby Peak, interpreted as the base of the CRMS (James, 1990). Elsewhere, thinner marble layers are isoclinally folded into all other Archean to Paleoproterozoic units, apparently occurring at multiple tectonostratigraphic positions. Thickest near Ruby Peak, where the apparent thickness is about 3,150 ft (960 m).

XAci ***Iron formation (Paleoproterozoic? to Archean?)***—Rusty-brown-weathering iron formation, with alternating layers of quartz and magnetite. Rarely exposed, mostly near the Kelly Mine (James, 1990). Mapped where two or more beds are present, following James (1990). Thickness less than 100 ft (30 m).

XAcq ***Quartzite (Paleoproterozoic? to Archean?)***—Vitreous white to green micaceous quartzite with uncommon biotite and garnet. Mapped where outcrops of more than approximately 10 ft (3 m) thick can be traced considerable distances. Thickness less than 50 ft (15 m).

XAam **Amphibolite (Paleoproterozoic to Archean)**—Foliated to massive, medium- to coarse-grained black and white, brownish-weathering hornblende–plagioclase ± garnet amphibolite (45.0 wt. percent SiO_2, fig 6; Mosolf and others, 2023b). Nearly equal parts amphibole and plagioclase, giving it a characteristic "salt and pepper" appearance. Coarse quartz stringers are common. Epidote, actinolite, diopside, and chlorite are uncommon. Contains rare, localized peridotite outcrops with abundant olivine, pyroxene, and serpentine. Forms resistant outcrops in lenses, pods, and boudins. Whole-rock geochemistry is similar to tholeiitic basalt composition, suggesting a mafic igneous rock protolith (Wilson, 1981; James, 1990). Commonly interlayered with the other Archean units, but only mapped where thickness exceeds several meters.

Adg **Dillon Gneiss (Archean)**—Foliated, gray-white to pink, reddish-brown-weathering, felsic to intermediate microcline–quartz–plagioclase ± biotite ± garnet ± hornblende gneiss and migmatite with interlayered black, coarse- to medium-grained amphibolite. Minor granite (quartz–microcline) pegmatite dikes, intrusions, and gneisses and quartz–plagioclase ± garnet leucogneiss. Leucogneiss is often mylonitized, with quartz and feldspar ribbons defining a lineation and foliation. Generally recessive, forming sparsely vegetated slopes. Rare quartzite and marble interbeds of a few meters thick. Lack of schist differentiates the Dillon Gneiss from the CRMS. In the southwestern Ruby Range, average composition of the Dillon Gneiss is granitic, with a mean of 74 wt. percent SiO_2 (James, 1990), with microcline, quartz, and plagioclase being the dominant minerals (Garihan and Williams, 1976). The wide range of lithologic variation observed on the outcrop scale may represent a complex sedimentary, volcanic, and igneous protolith (James and Hedge, 1980; James, 1990). U-Pb dating of zircon yields a weighted mean age of 2,453 ± 26 Ma (fig. 7C). Th/U values below 0.1 suggest this age represents Paleoproterozoic metamorphism (Brennan and others, in prep.). The upper contact with the overlying marble is generally sharp, with local infolding of the two units. At least 7,500 ft (2,290 m) thick.

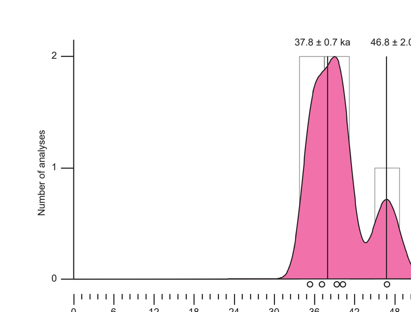

Figure 2. Probability density and histogram plot for boulders collected on the Laurin Canyon fan (Qafy) with corresponding cosmogenic ^{10}Be surface exposure age model results in thousands of years (ka).

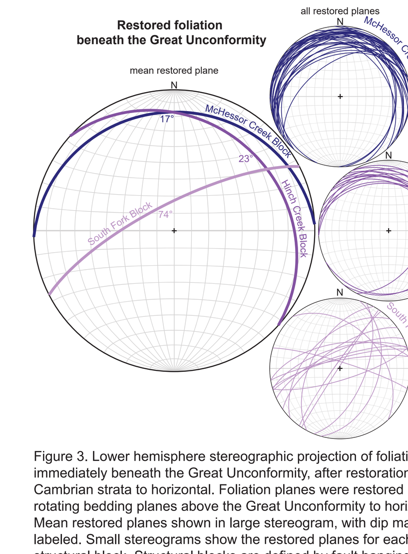

Figure 3. Lower hemisphere stereographic projection of foliation planes immediately beneath the Great Unconformity, after restoration of Cambrian strata to horizontal. Foliation planes were restored by rotating bedding planes above the Great Unconformity to horizontal. Mean restored planes shown in large stereograph, with dip magnitude labeled. Small stereograms show the restored planes for each structural block. Structural blocks are defined by fault hanging walls.

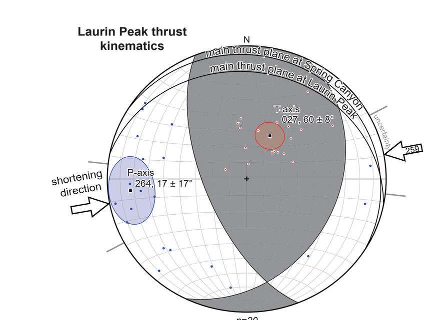

Figure 4. Lower hemisphere stereographic projection of calculated P- and T-axes and synthetic focal mechanism, based on measured slickenlines and minor faults related to the Laurin Peak and adjacent Spring Canyon thrusts. Measured main thrust planes shown by great circles. Ellipse shows 2σ-uncertainty envelope, with inferred shortening direction shown as arrow. Data is consistent with thrusting directed west-southwest (azimuth, 259) followed by tilting to the north.

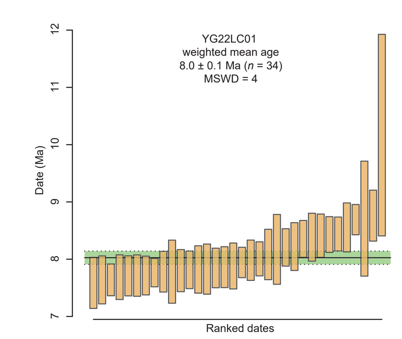

Figure 5. Weighted mean age of U-Pb zircon dates from sandy ash beds within the Sixmile Creek Formation (Tsc) near the Ruby Range northern border fault. Boxes show age and 2σ-uncertainty envelope for individual grains with <10% discordance, ranked by date.

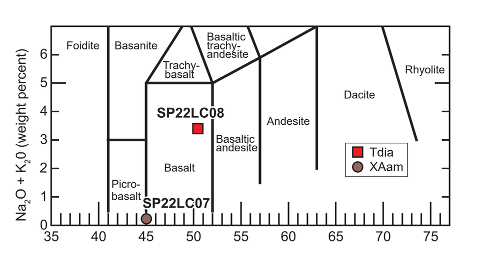

Figure 6. Whole-rock geochemical data from igneous (Tdia) and meta-igneous (XAam) rocks plotted on a total alkali silica classification diagram (after Le Bas and others, 1986). Plotted values are normalized to 100%.

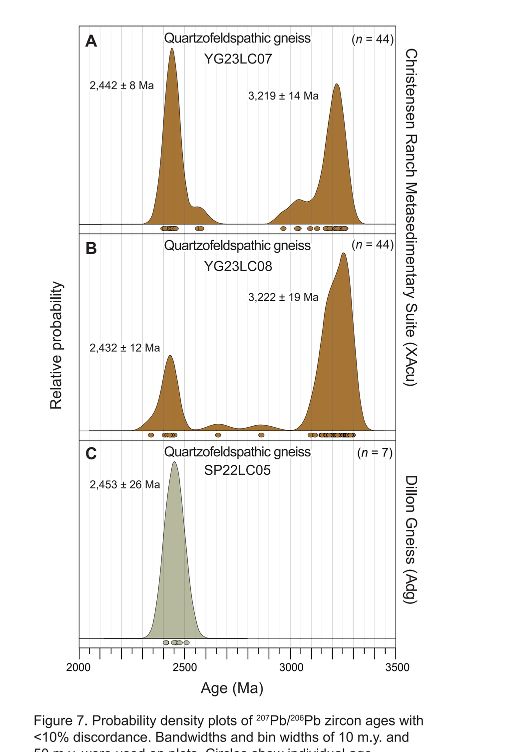

Figure 7. Probability density plots of $^{207}Pb/^{206}Pb$ zircon ages with <10% discordance. Bandwidths and bin widths of 10 m.y. and 50 m.y. were used on plots. Circles show individual age analyses. See table 2 for more information regarding weighted mean ages. Data reported in Mosolf and others (2023a), and Brennan and others (in prep.).

Table 1. Cosmogenic ^{10}Be sample data and modeled surface exposure ages.

Sample	Lat	Long	Elev (m)	Sample Thickness (cm)[a]	Quartz Mass (g)	Shield Correction[b]	$^{10}Be/^{9}Be$ ($x10^{-14}$)[c]	^{10}Be Concentration ($x10^3$ atoms/g SiO_2)[d]	Age (ka)[e,f]
Laurin Canyon fan: Qafy									
YG23LC09	45.3449	-112.1768	1693	1.50	25.00	0.974272	121.2 ± 1.8	623.35 ± 9.28	37.1 ± 1.5
YG23LC10	45.3447	-112.1770	1695	2.50	04.34	0.996478	27.0 ± 0.5	802.80 ± 1.51	46.8 ± 2.0
YG23LC11	45.3441	-112.1773	1698	1.75	25.00	0.996478	117.9 ± 1.6	607.15 ± 8.11	35.3 ± 1.4
YG23LC12	45.3426	-112.1789	1711	1.75	25.00	0.996478	136.4 ± 1.8	702.36 ± 9.36	40.2 ± 1.6
YG23LC13	45.3422	-112.1782	1713	2.75	25.00	0.995440	131.8 ± 1.8	680.12 ± 9.09	39.3 ± 1.6

Note: [a] Sample thickness represents the average sampling interval of material modeled for ^{10}Be exposure.
[b] Geometric shielding correction using CRONUS online calculator that includes strike and dip of the sampled surface.
[c] All uncertainties reported at 1σ. Blank corrected $^{10}Be/^{9}Be$ ratios. Total measurement uncertainty for the ^{10}Be concentration includes the uncertainty in the ^{9}Be carrier concentration, AMS measurement uncertainty, and uncertainty in the process blank correction. Combined, these uncertainties totaled to within 2% or 1σ.
[d] Ages reported using LSDn (Nuclide-dependent scaling age models by Lifton-Stato-Dunai; Lifton and others, 2014).
[e] Assumed value of zero erosion rates for stable and very resistant quartzite boulders.
[f] Age results generated by CRONUS-Earth online calculators (Balco and others, 2008), and using Promontory Point production rate calibration (Lifton and others, 2015). https://hess.ess.washington.edu/

Table 2. U-Pb zircon geochronology.

Sample	Lithology	Unit	Latitude (°N)	Longitude (°W)	No. of Spot Analyses[a]	Weighted Mean Age (Ma)	2σ	MSWD
YG22LC01	sandy ash beds	Tsc	45.3025	-112.1468	34/34	8.0	0.1	4.0
SP22LC05	quartzofeldspathic gneiss	Adg	45.3010	-112.2313	7/7	2452.5	25.9	4.0
YG23LC07	quartzofeldspathic gneiss	XAcu	45.2813	-112.1266	18*/44	2441.6	8.1	0.6
YG23LC07	quartzofeldspathic gneiss	XAcu	45.2813	-112.1266	18/44	3219.3	14.0	3.5
YG23LC08	quartzofeldspathic gneiss	XAcu	45.2799	-112.1328	8*/44	2431.6	12.1	0.7
YG23LC08	quartzofeldspathic gneiss	XAcu	45.2799	-112.1328	33/44	3222.1	18.6	11.0

Note: Reported ages are the weighted mean of the ^{207}Pb corrected $^{206}Pb/^{238}U$ ages for dates <1400 Ma, and $^{206}Pb/^{238}U$ ages for dates >1400 Ma. Only dates with <10% discordance were used in age calculations. MSWD is the Mean Square Weighted Deviation. Reported 2σ-uncertainties take into account overdispersion. Zircon separates were prepared at the MBMG and analyzed by LA-ICPMS at the University of California, Santa Barbara. Latitudes and longitudes are in the 1984 World Geodetic Survey (WGS84) datum.
[a] Numerator denotes the number of spot analyses used to calculated weighted mean age; denominator denotes the total number of concordant analyses in the sample.
*Outlier was not included in weighted mean age calculation.

REFERENCES

Balco, G., Stone, J.O., Lifton, N.A., and Dunai, T.J., 2008, A complete and easily accessible means of calculating surface exposure ages or erosion rates from ^{10}Be and ^{26}Al measurements: Quaternary Geochronology, v. 3, p. 174–195.
Brennan, D., Parker, S.D., Mosolf, J.G., and Kylander-Clark, A., In prep, U-Pb geochronology data from rock samples collected in the Dillon, Polson, and Wisdom 30′ x 60′ quadrangles, western Montana, 2022–2023: Montana Bureau of Mines and Geology Analytical Dataset.
Bush, J.H., Thomas, R.C., and Pope, M.C., 2012, Sauk megasequence deposition in northeastern Washington, northern Idaho, and western Montana, *in* Derby, J.R., Fritz, R.D., Longacre, S.A., Morgan, W.A., and Sternbach, C.A., eds., The great American carbonate bank: The geology and economic resources of the Cambrian-Ordovician Sauk megasequence of Laurentia: American Association of Petroleum Geologists Memoirs, v. 98, p. 751–768.
Cramer, M., 2015, Proterozoic tectonometamorphic evolution of the Ruby Range, SW Montana, USA: Insights from phase equilibria modeling and in situ monazite petrochonology: Missoula, University of Montana, M.S. thesis, 120 p., scale 1:24,000.
di Pasquo, M., Grader, G.W., Warren, A., Rice, B., Isaacson, P., and Doughty, P.T., 2017, Palynologic delineation of the Devonian-Carboniferous boundary, West-Central Montana, USA: Palynology, v. 41, no. S1, p. 189–220.
Dorobek, S.L., Reid, S.K., Elrick, M., Bond, G.C., and Kominz, M.A., 1991, Subsidence across the Antler foreland of Montana and Idaho: Tectonic versus eustatic effects: Kansas Geological Survey Bulletin, v. 233, p. 232–251.
Garihan, J.M., and Williams, K., 1976, Petrography, modal analyses and origin of Dillon quartzo-feldspathic and pre-Cherry Creek gneisses, Ruby Range, southwestern Montana: Northwest Geology, v. 5, p. 42–49.
Harms, T.A., and Baldwin, J.A., 2023, Paleoproterozoic geology of SW Montana: Implications for the paleogeography of the Wyoming craton and for the consolidation of Laurentia, *in* Whitmeyer, S.J., Williams, M.L., Kellett, D.A., and Tikoff, B., eds., Laurentia: Turning points in the evolution of a continent: Geological Society of America Memoirs, v. 220, p. 65–79.
James, H.L., and Wier, K.L., 1961, Geologic map of the Kelly iron deposit, Madison County, Montana: U.S. Geological Survey Open-File Report OF-61-76, scale 1:2,400.
James, H.L., and Wier, K.L., 1972, Geologic map of the Kelly iron deposit, sec. 25, T. 6 S., R. 5 W., Madison County, Montana: U.S. Geological Survey Miscellaneous Field Studies Map MF-349, scale 1:2,400.
James, H.L., and Hedge, C.E., 1980, Age of the basement rocks of southwest Montana: Geological Society of America Bulletin, v. 91, p. 11–15.
James, H.L., 1990, Precambrian geology and bedded iron deposits of the southwestern Ruby Range, Montana, with a section on the Kelly iron deposit of the northeastern Ruby Range: U.S. Geological Survey Professional Paper, v. 1495, 39 p., 2 plates, scale 1:4,600 and 1:24,000.
Jones, C.L., 2008, U-Pb geochronology of monazite and zircon in Precambrian metamorphic rocks from the Ruby Range, SW Montana: Deciphering geological events that shaped the NW Wyoming province: Kent, Ohio, Kent State University, M.S. thesis, 119 p.
Karasevich, L.P., 1980, Structure of the Pre-Beltian metamorphic rocks of the northern Ruby Range, southwestern Montana: State College, Penn State University, M.S. thesis, 172 p., 2 plates, scale 1:24,000.
Karasevich, L.P., Garihan, J.M., Dahl, P.S., and Okuma, A.F., 1981, Summary of Precambrian metamorphic and structural history, Ruby Range, Southwest Montana, *in* Tucker, T.E., ed., 1981 Montana Geological Society Field Conference and Symposium to Southwest Montana, v. 26, p. 225–238.
Lifton, N., Sato, S., and Dunai, T.J., 2014, Scaling in situ cosmogenic nuclide production rates using analytical approximations to atmospheric cosmic-ray fluxes, Earth and Planetary Science Letters, v. 386, p. 149–160, https://doi.org/10.1016/j.epsl.2013.10.052.
Lifton, N., Caffee, C., Finkel, R., Marrero, S., Nishiizumi, K., Phillips, F. M., Goehring, B., Gosse, J., Stone, J., Schaefer, J., Theriault, B., Jull, A.J. T., and Fifield, K., 2015, In situ cosmogenic nuclide production rate calibration for the CRONUS-Earth project from Lake Bonneville, Utah, shoreline features, Quaternary Geochronology, v. 26, p. 56-69, https://doi.org/10.1016/j.quageo.2014.11.002.
Link, P.K., Todt, M.K., Pearson, D.M. and Thomas, R.C., 2017, 500–490 Ma detrital zircons in Upper Cambrian Worm Creek and correlative sandstones, Idaho, Montana, and Wyoming: Magmatism and tectonism within the passive margin: Lithosphere, v. 9, no. 6, p. 910–926.
Mosolf, J.G., Brennan, D., and Kylander-Clark, A., 2023a, U-Pb geochronology data from rock samples collected in the Dillon, Ennis, Gardiner, Hamilton, Hebgen Lake, and Wisdom 30′ x 60′ quadrangles, western Montana, 2022–2023: Montana Bureau of Mines and Geology Analytical Dataset 5.
Mosolf, J.G., Brennan, D., Gavillot, Y., Parker, S., and Sears, J., 2023b, Major oxide and trace element analyses of rock samples collected in the Dillon and Hamilton 30′ x 60′ quadrangles, southwest Montana: Montana Bureau of Mines and Geology Analytical Dataset 2.
Ruppel, E.T., O'Neil, J.M., and Lopez, D.A., 1983, Preliminary geologic map of the Dillion 1° X 2° quadrangle, Montana: U.S. Geological Survey Open-File Report OF-83-168, scale 1:250,000.
Ruppel, E.T., O'Neill, J.M., and Lopez, D.A., 1993, Geologic map of the Dillon 1° x 2° quadrangle, Idaho and Montana: U.S. Geological Survey Miscellaneous Investigations Series Map I-1803-H, scale 1:250,000.
Sandberg, C.A., 1965, Nomenclature and correlation of lithologic subdivisions of the Jefferson and Three Forks formations of southern Montana and northern Wyoming: U.S. Geological Survey Bulletin 1194-N, 18 p.
Sando, W.J., and Dutro, J.T., 1974, Type sections of the Madison Group (Mississippian) and its subdivisions in Montana: U.S. Geological Survey Professional Paper, v. 842, 22 p., 1 plate.
Sando, W.J., and Sandberg, C.A., 1985, Revision of Mississippian Stratigraphy, Northern Tendoy Mountains, Southwest Montana: U.S. Geological Survey Bulletin 1656, p. A1–A9.
Schmidt, C.J., and J.M. Garihan, 1983, Laramide tectonic development of the Rocky Mountain foreland of Southwestern Montana, *in* Lowell, J.D., ed., Rocky Mountain foreland basins and uplifts: Rocky Mountain Association of Geologists, p. 271–294.
Schmidt, C.J., O'Neill, J.M., and Brandon, W.C., 1988, Influence of Rocky Mountain foreland uplifts on the development of the frontal fold and thrust belt, southwestern Montana, *in* Schmidt, C.J., and Perry, W.J., eds., Interaction of the Rocky Mountain foreland and the Cordilleran thrust belt: Geological Society of America Memoirs, v. 17, p. 171–202.
St. Jean, Z.C., and Teeter, D.R., 2004, Geologic map of the Ruby Dam area, southwest Montana: Montana Bureau of Mines and Geology Open-File Report, v. 488, scale 1:48,000.
Stickney, M.C., 2022, Earthquakes and seismographic monitoring in Montana, *in* Metesh, J., Geology of Montana: Montana Bureau of Mines and Geology Special Publication 122, available at http://www.mbmg.mtech.edu/pubs/GeologyofMontana/
Stickney, M.C., Haller, K.M., and Machette, M.N., 2000, Quaternary faults and seismicity in Western Montana: Montana Bureau of Mines and Geology Special Publication 114, 1 sheet, scale 1:750,000.
Thomas, R.C., 2007, A field guide to the Cambrian section at Camp Creek, southwest Montana: Northwest Geology, v. 36, p. 231–244.
Tysdal, R.G., 1970, Geology of the north end of the Ruby Range, southwestern Montana: Missoula, University of Montana, Ph.D. dissertation, 187 p., 6 plates, scale 1:24,000.
Tysdal, R.G., 1976, Geologic map of the northern part of Ruby Range, Madison County, Montana: U.S. Geological Survey Miscellaneous Investigations Series Map I-951, scale 1:24,000.
Tysdal, R.G., 1981, Foreland deformation in the northern part of the Ruby Range of Southwest Montana, *in* Tucker, T.E., ed., 1981 Montana Geological Society Field Conference and Symposium to Southwest Montana, v. 26, p. 215–224.
Tysdal, R.G., Lee, G.K., Hassemer, J.H., Hanna, W.F., Schmauch, S.W., and Berg, R.B., 1987, Mineral resources of the Ruby Mountains Wilderness Study Area, Madison County, Montana: U.S. Geological Survey Bulletin, v. 1724, 22 p., 1 plate, scale 1:24,000.
Wilson, M.L., 1981, Origin of Archean lithologies in the southern Tobacco Root and northern Ruby Range of southwestern Montana, *in* Tucker, T.E., ed., 1981 Montana Geological Society Field Conference and Symposium to Southwest Montana, v. 26, p. 37–43.
Wooden, J.L., Vitaliano, C.J., Koehler, S.W., and Ragland, P.C., 1978, The late Precambrian mafic dikes of the southern Tobacco Root Mountains, Montana: Geochemistry, Rb-Sr geochronology and relationship to Belt tectonics: Canadian Journal of Earth Science, v. 15, p. 467–479.

Montana Bureau of Mines and Geology

Geologic Map 98

Geologic Map of the Laurin Canyon 7.5′ Quadrangle, Madison County, Montana

Stuart D. Parker and Yann G. Gavillot

2024
https://doi.org/10.59691/WMJR3264